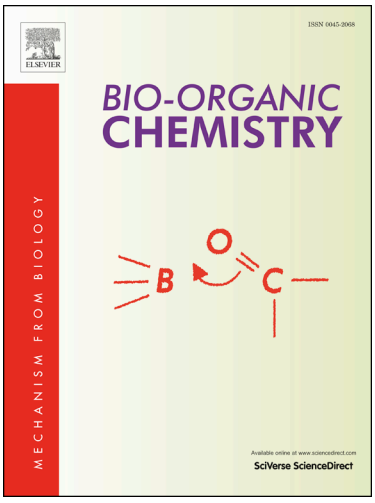

Oxidation at C-16 enhances butyrylcholinesterase inhibition in lupane triterpenoids

María Julia Castro, Victoria Richmond, María Belén Faraoni, Ana Paula Murray

PII: S0045-2068(18)30197-4
DOI: https://doi.org/10.1016/j.bioorg.2018.05.012
Reference: YBIOO 2365

To appear in: *Bioorganic Chemistry*

Received Date: 1 March 2018
Revised Date: 7 May 2018
Accepted Date: 14 May 2018

Please cite this article as: M. Julia Castro, V. Richmond, M. Belén Faraoni, A. Paula Murray, Oxidation at C-16 enhances butyrylcholinesterase inhibition in lupane triterpenoids, *Bioorganic Chemistry* (2018), doi: https://doi.org/10.1016/j.bioorg.2018.05.012

Oxidation at C-16 enhances butyrylcholinesterase inhibition in lupane triterpenoids.

María Julia Castro[a], Victoria Richmond[b], María Belén Faraoni[a], Ana Paula Murray[a,]*

[a] *INQUISUR-CONICET, Departamento de Química, Universidad Nacional del Sur, Av. Alem 1253, B8000CPB Bahía Blanca, Argentina*
[b] *UMYMFOR (CONICET-UBA), Departamento de Química Orgánica, Facultad de Ciencias Exactas y Naturales, Universidad de Buenos Aires, Ciudad Universitaria, Pabellón 2, 1428 Buenos Aires, Argentina*

Corresponding author e-mail: apmurray@uns.edu.ar

Abstract

A set of triterpenoids with different grades of oxidation in the lupane skeleton were prepared and evaluated as cholinesterase inhibitors. Allylic oxidation with selenium oxide and Jones's oxidation were employed to obtain mono-, di- and tri-oxolupanes, starting from calenduladiol (**1**) and lupeol (**3**). All the derivatives showed a selective inhibition of butyrylcholinesterase over acetylcholinesterase (BChE *vs.* AChE). A kinetic study proved that compounds **2** and **9,** the more potent inhibitors of the series, act as competitive inhibitors. Molecular modeling was used to understand their interaction with BChE, the role of carbonyl at C-16 and the selectivity towards this enzyme over AChE. These results indicate that oxidation at C-16 of the lupane skeleton is a key transformation in order to improve the cholinesterase inhibition of these compounds.

Keywords: Cholinesterase inhibitors, Lupane derivatives, Triterpenoids, Molecular modeling

1. Introduction

Cholinesterase inhibition is the most accepted therapeutic strategy for the treatment of Alzheimer's disease (AD), a progressive neurodegenerative disorder that affects the elderly population and causes memory impairment and cognitive deficit [1–3]. The inhibition of acetylcholinesterase (AChE), the enzyme that catalyzes the hydrolysis of the neurotransmitter

acetylcholine, can alleviate AD symptoms by improving cholinergic functions in AD patients. In the healthy brain, the enzyme butyrylcholinesterase (BChE) is also involved in the metabolic degradation of acetylcholine, although the cholinesterase activity of AChE is much higher than that of BChE [4, 5]. In AD patients, the AChE/BChE ratio depends on the brain region and the stage of the disease progression. BChE can compensate AChE activity when its levels are decreased. Since BChE activity increases as AD progresses, this enzyme may also play an important role in cholinergic dysfunction, particularly at the later stages of AD [6].

As part of our research program focused on the discovery of new cholinesterase inhibitors, we recently reported the synthesis of several analogs of calenduladiol (lup-20(29)-en-3β,16β-diol, **1**) and the selective BChE inhibition observed for 3,16-dioxolup-20(29)-en-30-al (**2**) (Figure 1) [7]. Taking into account those results, in this work we further investigated the role of the oxidation of the lupane skeleton in the BChE inhibition. For that purpose, we chose two natural compounds, lupanes **1** and **3**, as starting material and carried out chemical transformations that provided a set of lupane derivatives with selective oxidation at C-3, C-16, and/or C-30. All the derivatives were evaluated as cholinesterase inhibitors, and a kinetic study was performed for the two more potent BChE inhibitors. Also, the key binding interactions between these compounds and BChE was studied through docking modelization.

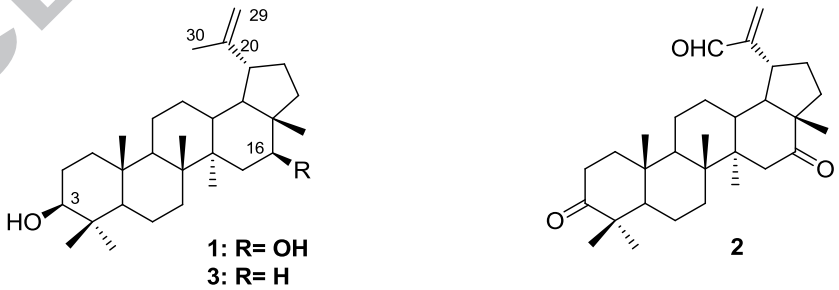

Figure 1. Structure of calenduladiol (**1**), 3,16-dioxolup-20(29)-en-30-al (**2**) and lupeol (**3**).

2. Results and discussion

2.1 Chemistry

Our previous findings revealed that trioxolupane (**2**) may provide a useful template for the development of new lupane derivatives with improved and selective BChE inhibition [7]. A set of 11 lupane derivatives were prepared by different oxidation strategies in order to obtain analogs selectively oxidized at the same three positions as on compound **2**, that is, positions 3, 16, and 30 of the lupane skeleton. Cholinesterase inhibition was determined for each compound and the results were analyzed with the aid of molecular modeling.

Taking into account our previous results, we designed a strategy to obtain a set of compounds with different grades of oxidation in the lupane skeleton, starting from two natural triterpenes, calenduladiol (**1**) and lupeol (**3**), both isolated for this purpose from *Chuquiraga erinacea* subsp *erinacea* (Asteraceae) following a procedure already reported [8]. Allylic oxidation with selenium oxide and Jones's oxidation were employed to obtain mono-, di- and tri-oxolupanes that would allow us to determine which carbonyl group is necessary for enzyme inhibition. In order to analyze the role of the hydroxyl/carbonyl groups at C-3, C-16, and C-30, we have carried out the transformations shown in Scheme 1 and Scheme 2.

Initially, lupeol (**3**) was treated with Jones reagent to obtain lupenone (**4**) (lup-20(29)-en-3-one) with excellent yield (93%). Starting also from **3**, allylic oxidation at C-30 led us to α,β-unsatured aldehyde **5** (3β-hydroxy-lup-20(29)-en-30-al). Then, oxidation of compound **5** with Jones reagent rendered 3,30-dioxolupane **6** (3-oxo-lup-20(29)-en-30-al) (Scheme 1).

The alternative route for preparing compound **6** by treating intermediate **4** with selenium oxide was discarded on the basis of the results reported by Gutierrez-Nicolás *et al.* in the allylic oxidation of lupenone, where this reaction also rendered the α,β-unsaturated ketone at ring A together with the desired oxidation of C-30 [9].

Compounds **4**, **5**, and **6** were purified by column chromatography and identified by comparison of their spectroscopic data with those reported in the literature. Ketone **4** has been found as a natural compound in different plant species, and was also obtained by synthesis and used in further preparation of other synthetic analogs [10–15]. Compound **6** was identified by Mutai *et al* as a secondary metabolite found in *Acacia mellifera* [11]. Spectroscopic data of **5** were in agreement with those reported by Burns *et al* [16].

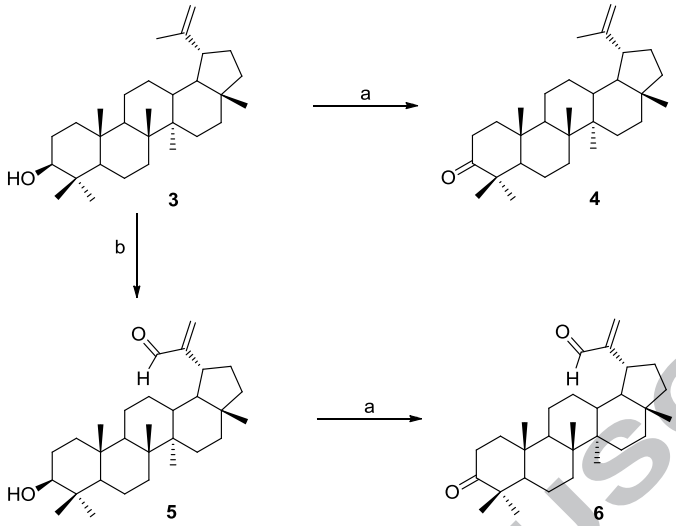

Scheme 1. Preparation of compounds **4**–**6**. Reagents and conditions: (a) Jones reagent, acetone; (b) SeO_2, EtOH, reflux.

Following the same strategy but starting from calenduladiol (**1**), we were able to prepare compounds **7** (3β,16β-dihydroxy-lup-20(29)-en-30-al) and **2** (3,16-dioxo-lup-20(29)-en-30-al) (Scheme 2). The oxidation of **1** directly with Jones reagent led us to compound **8** (3,16-dioxo-lup-20(29)-ene) as the major product, together with the partially oxidized analogs, **9** (3β-hydroxy-lup-20(29)-en-16-one) and **10 (**16β-hydroxy-lup-20(29)-en-3-one), in 42:24:34 ratio, respectively (Scheme 2). Compounds **8**–**10** were separated by column chromatography. Then, allylic oxidation of compound **9** rendered compound **11** (3β-hydroxy-16-oxo-lup-20(29)-en-30-al, 47.2% yield), while compounds **12** (16β-hydroxy-3-oxo-lup-20(29)-en-30-al, 13.7% yield) and **13** (16β-hydroxy-3-oxo-lup-1,20(29)-dien-30-al, 18.7 % yield) were obtained from **10** at the same experimental conditions (Scheme 2).

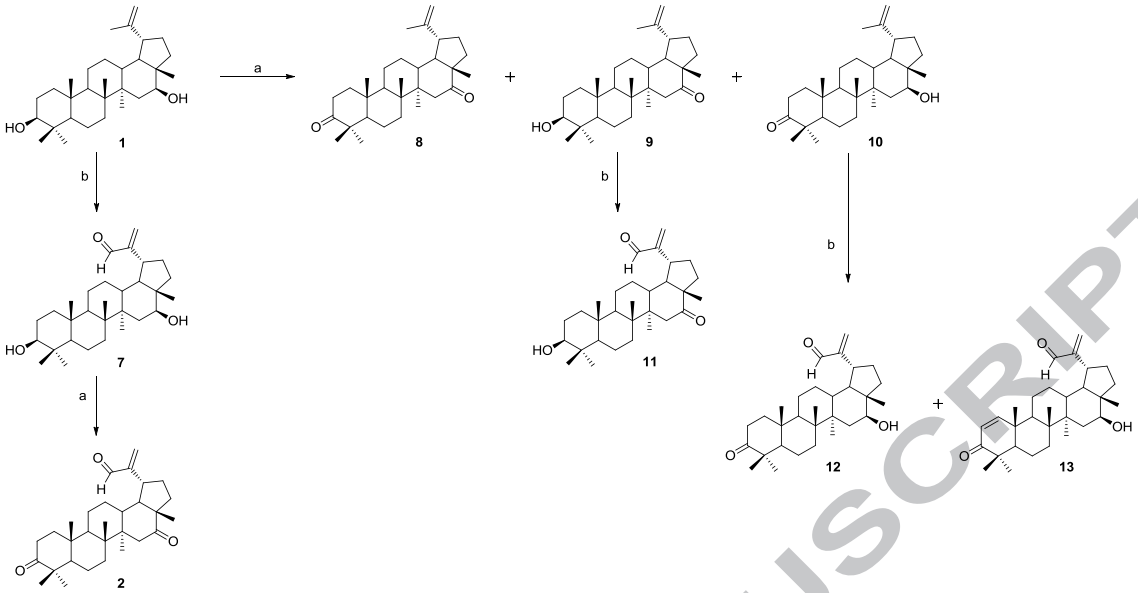

Scheme 2. Preparation of compounds **2**, **7**–**13**. Reagents and conditions: (a) Jones reagent, acetone; (b) SeO_2, EtOH, reflux.

The synthesis of **11** and **12** starting from compound **7** was theoretically possible. When we tried to do so by careful addition of Jones reagent onto a cooled solution of **7**, the TLC showed the presence of three compounds. The chromatographic separation of the reaction crude rendered starting compound **7** as the major product, together with a mixture of **11** and **12** that could not be separated. These results prompted us to try the alternative route described previously (Scheme 2), even though we could expect the formation of some elimination product in ring *A* [9]. Taking into account that ketones **9** and **10** were obtained as minor byproducts in the synthesis of compound **8**, reaction conditions were optimized in order to promote the formation of those products instead of **8**. After careful column chromatography we were able to obtain ketones **9** and **10** in adequate amounts to approach the next step, the allylic oxidation of each one separately. Thus, we were able to obtain compounds **11** and **12**, both with the α,β-unsatured aldehyde moiety in the side chain, but with selective oxidation of C-3 or C-16. As it was expected, compound **13** was also obtained, together with compound **12**, but their separation was successfully achieved by column chromatography.

Lupanes **2**, **7**, and **8** were identified by comparison of their spectroscopic data with those reported in our previous work [7]. Ketone **10** presented ^{1}H and ^{13}C NMR spectra matching those

reported for the natural triterpenoid isolated from *Acacia cedilloi* (Fabaceae), known as resinone [17]. Compounds **9**, **11**, **12**, and **13** are, on the other hand, new lupane derivatives and were identified with the aid of NMR spectroscopy and MS spectrometry. Assignments of all carbon and relevant proton signals were achieved with the aid of mono- and bi-dimensional NMR experiments and comparison with NMR data of the known analogs and/or starting triterpenoids [7, 9, 17, 18].

2.2 Cholinesterase inhibition

The AChE and BChE inhibitory activity of compounds **4**–**13** was evaluated and compared to that of natural triterpenoids **1** and **3**, and compound **2**. AChE and BChE activities were measured *in vitro* by the spectrophotometric method developed by Ellman with slight modifications with tacrine as the reference inhibitor [19].

In a preliminary assay the inhibition percentage at a fixed concentration was determined for all the derivatives. Compounds **1**–**13** acted like weak AChE inhibitors with low inhibition percentages. On the other hand, compounds **2**, **8**, **9** and **11** showed better BChE inhibition than **1** under the same experimental conditions (Table 1). The concentration required for 50% BChE inhibition (IC_{50}) was then determined for these compounds. The results for cholinesterase inhibition are summarized in Table 1.

Table 1. Cholinesterase inhibition of compounds **1**-**13**

Compound	**AChE % Inhibition**[a]	**BChE % Inhibition**[a]	**IC_{50} (μM)**
1 [b]	8.1 ± 0.2	42.0 ± 0.8	**>200**
2 [b]	21.7 ± 1.2	86.5 ± 2.7	**21.5 ± 1.2**
3	21.3 ± 2.7	31.0 ± 2.2	**>200**
4	8.8 ± 1.2	10.2 ± 1.4	-
5	5.7 ± 0.4	3.2 ± 1.0	-
6	n.i. [c]	28.9 ± 3.1	-
7 [b]	43.5 ± 1.1	42.0 ± 4.4	**>200**
8	6.4 ± 0.3	61.4 ± 0.5	**154.6 ± 2.3**
9	40.2 ± 2.1	> 100	**28.9 ± 2.1**

10	12.6 ± 1.5	43.5 ± 0.9	**>200**
11	29.7 ± 0.8	> 100	**76.8 ± 0.3**
12	n.i. [c]	35.3	**>200**
13	n.i. [c]	44.6 ± 0.6	**>200**
tacrine [d]	-	-	**0.004 ± 0.001**

[a] at 200 μM, [b] From ref. 7, [c] n.i. : no inhibition detected, [d] reference inhibitor.

The best activity was observed for compound **2**, with three carbonyl groups in positions 3, 16 and 30, followed by compound **9** (3β-hydroxy-lup-20(29)-en-16-one). All the compounds bearing a 16-keto group were more effective inhibitors than the 16β-hydroxy analogs (**9** *vs*. **1**, **11** *vs*. **7**, **8** *vs*. **10**, **2** *vs*. **12**,) or the unsubstituted lupanes (**9** *vs*. **3**, **11** *vs*. **5**, **8** *vs*. **4**, **2** *vs*. **6**,) (Figure 2).

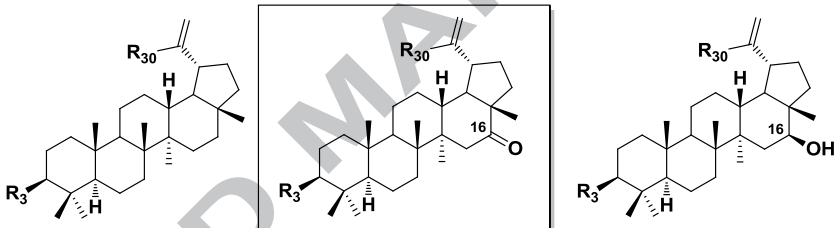

R-3	R-30	Compound	IC_{50} (μM)
OH	CH_3	3	>200
OH	CHO	5	-
=O	CH_3	4	-
=O	CHO	6	-

Compound	IC_{50} (μM)
9	28.9
11	76.8
8	154.6
2	21.5

Compound	IC_{50} (μM)
1	>200
7	>200
10	>200
12	>200

Figure 2. BChE inhibitors grouped according their substitution at C-16.

2.3 Kinetic characterization of BChE inhibition

Carbonyl compounds **2** and **9**, identified as the more effective BChE inhibitors of the series, were chosen for the determination of the inhibitor type kinetic study. Enzyme activity was evaluated at different fixed inhibitor concentrations and increasing substrate concentrations and, the data obtained was used to elucidate the enzyme inhibition mechanism. The results are illustrated in the form of Lineweaver–Burk plots (Figure 3). The double-reciprocal plots showed that the inhibitors have not effect on V_{max}, but increase K_m. The pattern of straight lines with intersecting *y* intercepts seen in Figure 3 is the characteristic signature of a competitive

inhibitor. Both **2** and **9**, interfere with the substrate binding to the enzyme. The analysis of these data with GraphPad Prism 5 showed a good fit with the competitive type inhibition. Estimated K_i were 51.16 µM for **9** and 32.70 µM for **2**. This kinetic study indicates that both **2** and **9** have affinity for the active site of the enzyme and compete with the substrate.

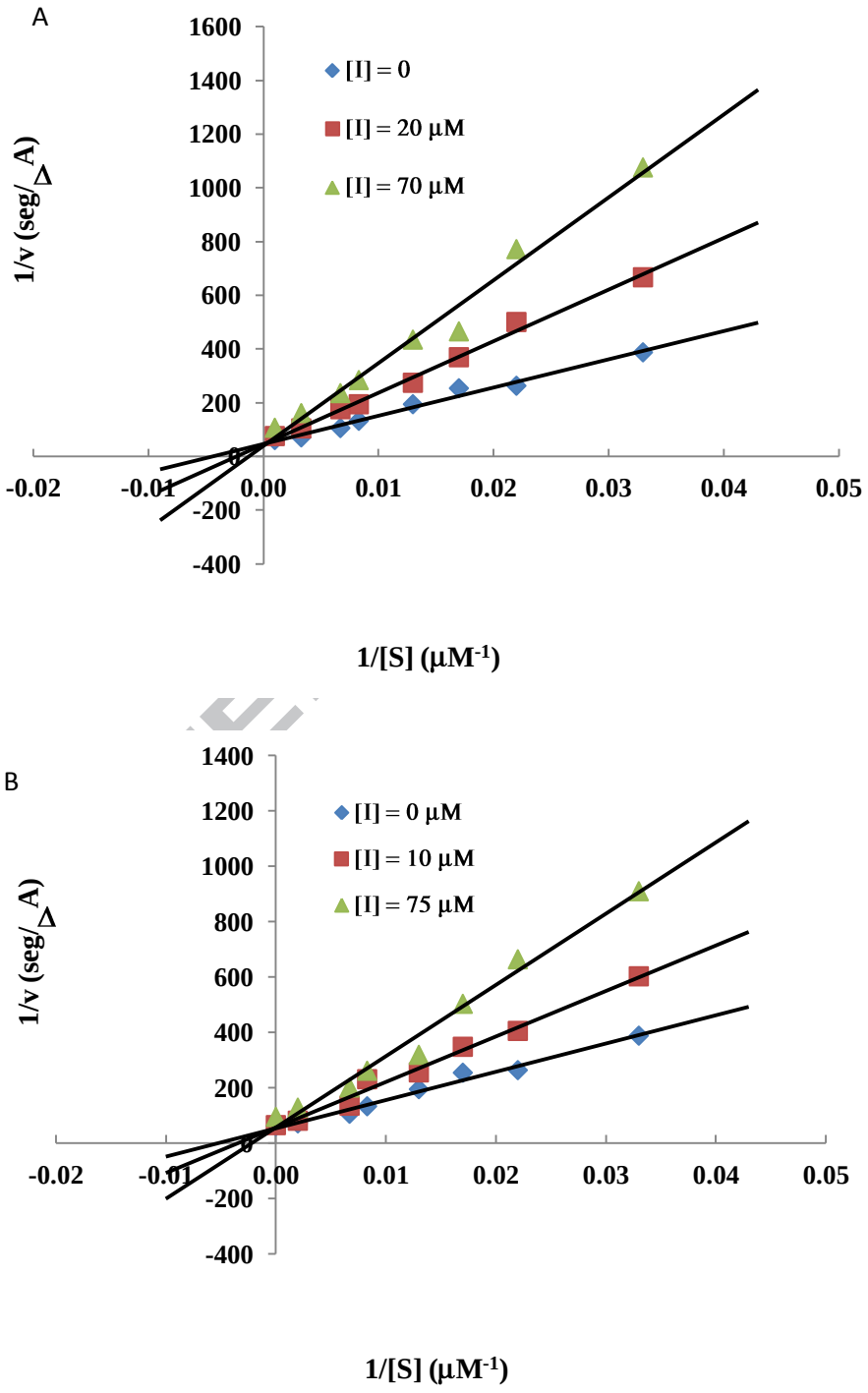

Figure 3. Lineweaver–Burk plots of the inhibition of BChE by compound **2** (A) and **9** (B) with butyrylthiocholine (S) as substrate.

2.4 Molecular modeling study

In order to understand the selective BChE inhibition of compounds **2** and **9** over AChE inhibition, molecular docking studies were performed with both cholinesterases to compare their affinities. Owing to the large volume of the BChE active-site gorge (200 $Å^3$ bigger than that of the AChE gorge), one or more molecules of water can be placed there in order to interact with the ligand, improving the interaction with the protein [20]. This difference in the dimension of the active-site gorge led us to implement a hydrated docking technique with the enzyme BChE [21].

When studying the binding mode and the interactions between these compounds and BChE, the best molecular docking conformation showed that compounds **2** and **9** penetrate the peripheral site through their *A* ring and bind the enzyme at the active site; both cases exhibit the triterpenoid buried deep into the gorge next to the residue SER198 (belonging to the catalytic triad), according to the competitive inhibition mechanism of the BChE that the *in vitro* experiments revealed.

The study permitted us to identify hydrophobic interactions inside the gorge as well as three hydrogen bonding interactions as stabilizing factors in the enzyme-inhibitor complex for both compounds. The hydrophobic interactions are depicted in Figure 4. Due to both compounds sharing the same position at the gorge of the enzyme, the figure only represents these interactions between the BChE and compound **2**. Regarding the hydrogen bonding, the carbonyl group at C-16 of compound **9** interacts with the hydroxyl group of THR 120 (2.30Å) and the carbonyl group of TRP82 (water mediated 2.05 and 2.27Å). Also, the hydroxyl group at C-3 in compound **9** is close to the carbonyl group of LEU286 (2.22Å) (Figure 5). Similarly, the carbonyl group at C-16 of **2** is involved in the same two hydrogen bonds as compound **9**, with the hydroxyl group of THR120 (2.22Å) and TRP82 water mediated (2.05 and 2.12Å). There is another water-bridged H-bond network between the carbonyl at C-30 and the residue ASN289 (2.05 and 2.40 Å). These interactions are shown in Figure 6. The importance of the carbonyl group at C-16 present in both compounds should be noted since both lone pairs of the oxygen

are involved in a hydrogen bond that strongly dock the compounds at the active site of the protein.

On the other hand, the molecular docking with the AChE revealed that although both compounds get into the enzyme in the same way they penetrate the BChE (through their ring *A*), both compounds are located at the peripheral aromatic site of the enzyme, and the main interactions that stabilized these compounds are hydrophobic. Additionally, compound **2** showed only one hydrogen bond between the carbonyl of C-30 and the NH of the amide group of PHE288.

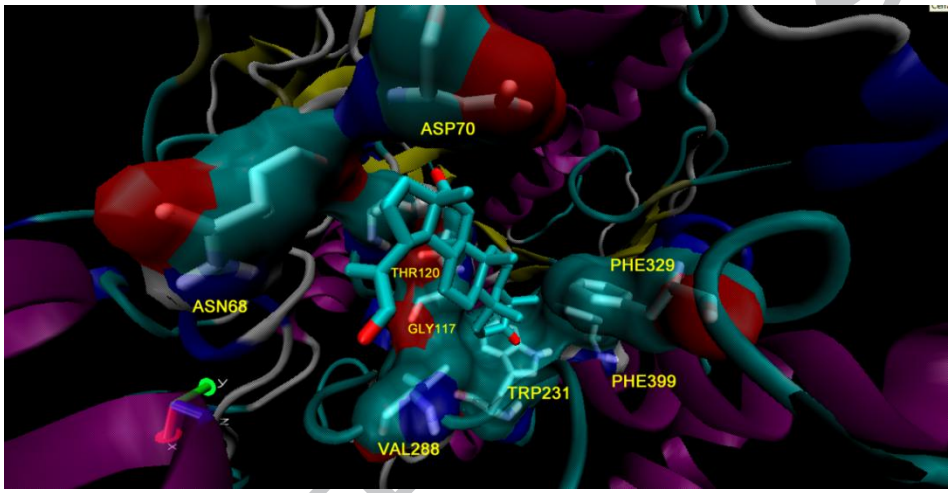

Figure 4. Hydrophobic interactions between compound **2** and the enzyme butyrylcholinesterase.

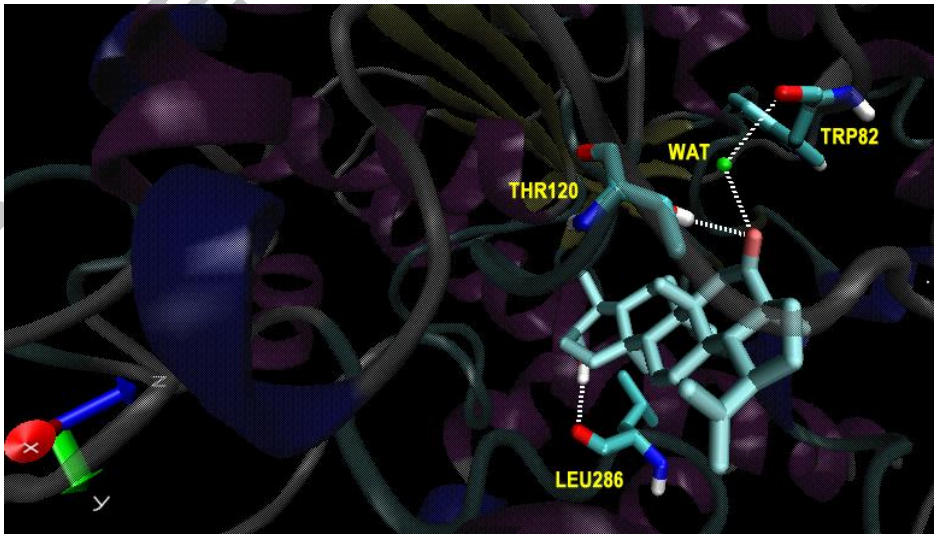

Figure 5. Hydrogen bonds between compound **9** and the enzyme BChE.

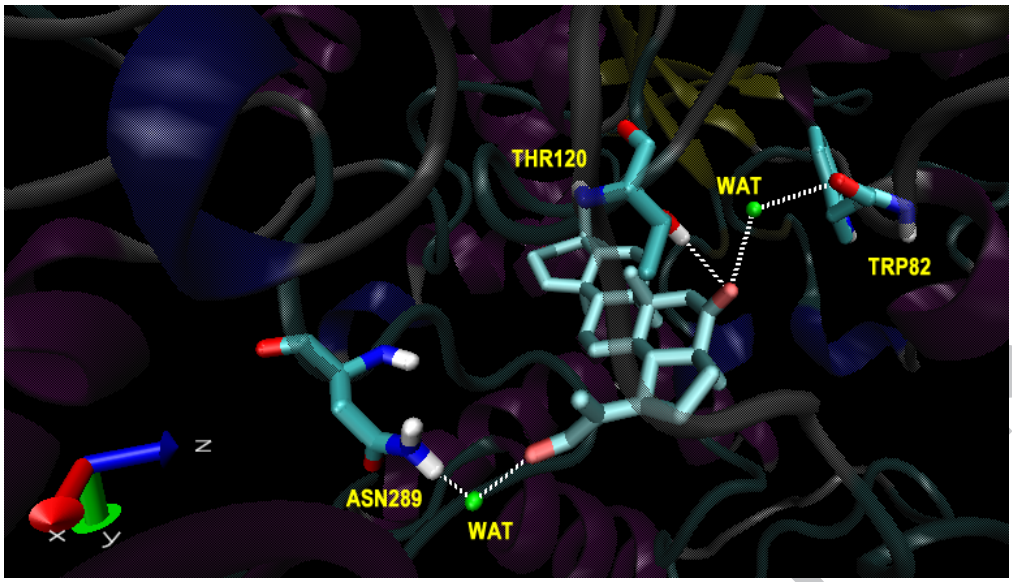

Figure 6. Hydrogen bonds between compound **2** and the enzyme BChE.

According to the results described for both compounds with the two cholinesterases, the stronger interaction between these triterpenoids and BChE is highlighted. This result clearly explains the molecular mechanism of the selectivity of these compounds toward the mentioned enzyme.

The docking studies allowed us to establish the orientation of the inhibitors relative to the BChE, as well as its conformation when bound to the enzyme. This study permitted us to identify hydrophobic interactions inside the gorge as well as hydrogen bonding interactions as the stabilizing factors in the enzyme-inhibitor complex. Moreover, this work allowed us to understand the molecular basis of the selectivity of these compounds toward the enzyme BChE.

Further molecular dynamics studies using this complex as the starting point are necessary to check the complex inhibitor-enzyme stability, to determinate if the enzyme undergoes structural rearrangements, and to verify the distances and angles observed in the interactions are within a suitable range.

3. Conclusions

Starting from calenduladiol (**1**) and lupeol (**3**), two natural triterpenoids, we have obtained a set of lupane-type compounds with keto groups at C-3, C-16, and/or C-30. Four new

semisynthetic triterpenoids were obtained and fully characterized, together with seven known ones, in order to understand the influence of the carbonyl group in the interaction of these compounds with AChE and BChE. Compounds **2** and **9** were identified as the most effective BChE inhibitors. A kinetic study indicated that **2** and **9** are able to bind to the enzyme in a competitive manner. The experimental results were explained by means of molecular modeling, which helps to understand the selectivity of these inhibitors towards BChE. Also, this study allowed us to identify hydrophobic interactions inside the gorge, as well as hydrogen bonding interactions as the stabilizing factors in the enzyme-inhibitor complex.

These results show that oxidation of C-16 is an efficient way to improve cholinesterase inhibition in this kind of inhibitor. Since compounds **2** and **9**, the most active in the series, can be further modified in the isopropenyl attached to ring *E*, they appear to be good candidates to explore the scope of this scaffold as potential lead compounds in the search of new anti-Alzheimer's drugs.

4. Experimental Section

4.1 General

Melting points were determined on a Fisher-Johns apparatus and are uncorrected. NMR measurements, including COSY, HSQC, HMBC experiments, were carried out on Bruker ARX300, Bruker Avance 400 and/or Bruker AMK 600 spectrometers. NMR spectra were recorded in $CDCl_3$. Chemical shifts are given in ppm (δ) with TMS as an internal standard. Electrospray ionization mass spectra (ESI-MS) were recorded using an Esquire 3000 ion trap mass spectrometer equipped with a standard ESI/APCI source. UV spectra were recorded on a JASCO V-630BIO spectrophotometer. Elemental analyses (C, H) were performed with EXETER ANALYTICAL, INC CE-440 Elemental Analyzer. IR spectra were recorded on a Perkin-Elmer Paragon 1000 FT-IR spectrometer.

Silica gel 60 (0.2–0.63 mm, Merck) was used for column chromatography. Silica gel 60 (200–425 mesh, Aldrich) was used for flash chromatography. Analytical TLC was performed

on Silicagel 60 F254 sheets (0.2 mm thickness, Merck). *p*-Anisaldehyde-acetic acid spray reagent and UV light (254 and 366 nm) were used for detection.

All chemicals and solvents were analytical grade and solvents were purified by general methods before being used. AChE from electric eel (type VI-S), 5,5 -dithiobis(2-nitrobenzoic acid) (DTNB), acetylthiocholine iodide (ATCI), butyrylthiocholine iodide (BTCI) and tacrine were purchased from Sigma. BChE (horse serum) was purchased from MP Biomedicals. Calenduladiol (**1**) and lupeol (**3**), used as starting materials for the preparation of compounds **2, 4**–**13**, were extracted from aerial parts of *C. erinacea* subsp. *erinacea* as previously described [8].

All derivatives were rigorously characterized by NMR spectroscopy and mass spectrometry. The NMR data of derivatives **2, 4**–**8** and **10** were identical to those previously reported [7, 11, 12, 17].

Compounds **9**, **11**–**13** are described here for the first time and bidimensional NMR spectra (COSY, HMBC, HSQC) were used for the unequivocal assignments of all carbons and representative protons.

*4.2 Preparation of 3,16-dioxo-lup-20(29)-en-30-al (**2**)*

To a solution of **7** (50.0 mg, 0.11 mmol) in acetone (3 mL) Jones reagent was added dropwise at 0 °C until the solution changed remained orange. The reaction was stirred for 30 min and quenched with *i*-PrOH (2 mL), filtered through Florisil and washed several times with AcOEt. The solvent was removed and the residue was purified by flash chromatography on silica gel with hexane/AcOEt (9:1) affording 12.9 mg (26%) of compound **2** as a white amorphous solid. Spectroscopic and spectrometric data of **2** were in agreement with those previously reported by our group [7]. ^{1}H NMR (600 MHz, $CDCl_3$) δ 0.89 (3H, s, H-27), 0.93 (3H, s, H-25), 1.02 (3H, s, H-24), 1.07 (3H, s, H-28), 1.13 (6H, s, H-23, H-26), 2.48 (1H, ddd, *J* = 8.6, 15.7, 15.9 Hz, H-19), 2.74 (1H, d, *J* = 13.8 Hz, H-15a), 5.98 (1H, br s, H-29a), 6.29 (1H, *br* s, H-29b), 9.52 (1H, s, H-30); ^{13}C NMR (150 MHz, $CDCl_3$) δ 217.9 (C-3), 215.4 (C-16), 194.8 (C-30), 156.2 (C-20), 133.3 (C-29), 56.9 (C-17), 54.8 (C-5), 49.2 (C-9, C-18), 47.7 (C-

14), 47.4 (C-4), 44.9 (C-15), 41.0 (C-8), 39.6 (C-1), 37.3 (C-13, C-19), 36.9 (C-10), 34.2 (C-2), 33.6 (C-7, C-22), 31.3 (C-12, C-21), 26.8 (C-23), 21.2 (C-11), 21.2 (C-24), 19.6 (C-6), 18.1 (C-28), 16.3 (C-26), 15.9 (C-25), 15.4 (C-27).

*4.3 Preparation of lup-20(29)-en-3-one (**4**)*

Compound **4** was prepared from **3** (50.0 mg, 0.12 mmol) following the same procedure described for the preparation of **2**. The crude material was chromatographed over flash silica gel with hexane/AcOEt (9:1) to afford 47.4 mg (95%) of compound **4** as a white amorphous solid. Spectroscopic and spectrometric data of **4** were identical to those reported for lupenone [11, 12]. ^{1}H NMR (300 MHz, $CDCl_3$) δ 0.83 (3H, s, H-28), 0.85 (3H, s, H-25), 0.94 (3H, s, H-27), 0.96 (3H, s, H-24), 1.03 (6H, s, H-23, H-26), 1.63-1.25 (27H, m), 2.41 (1H, m, H-19), 4.54 (1H, *br* s, H-29b), 4.67 (1H, *br* s, H-29a); ^{13}C NMR (75 MHz, $CDCl_3$) δ 218.0 (C-3), 150.8 (C-20), 109.5 (C-29), 55.0 (C-5), 49.9 (C-9), 48.3 (C-18), 48.0 (C-19), 47.4 (C-4), 43.1 (C-17), 43.1 (C-14), 40.9 (C-8), 40.1 (C-22), 39.7 (C-13), 38.2 (C-1), 36.9 (C-10), 35.7 (C-16), 34.2 (C-2), 33.7 (C-7), 29.9 (C-21), 27.5 (C-15), 26.8 (C-23), 25.2 (C-12), 21.6 (C-24), 21.1 (C- 11), 19.8 (C-30), 19.8 (C-6), 18.1 (C-28), 16.2 (C-26), 16.0 (C-25), 15.9 (C-27).

*4.4 Preparation of 3β-hydroxy-lup-20(29)-en-30-al (**5**)*

A solution of **3** (40.0 mg, 0.09 mmol) in EtOH (5 mL) was treated with SeO_2 (24.2 mg, 0.22 mmol). The reaction mixture was heated under reflux until the disappearance of the starting material was confirmed by TLC (24 h). Then, the reaction mixture was cooled and EtOH was removed under reduced pressure. The crude was treated with water (20 mL) and extracted with CH_2Cl_2 (3 x 30 mL). The combined organic extracts were dried over $MgSO_4$, filtered, and concentrated under reduced pressure. The residue was purified by column flash chromatography on silica gel with hexane/AcOEt (7:3) to afford 18.0 mg (44%) of compound **5** as a white crystalline solid. Compound **5** showed identical spectroscopic and spectrometric data to those previously reported [16]. ^{1}H NMR (300 MHz, $CDCl_3$) δ 0.66 (1H, d, J = 9.0 Hz, H-5), 0.75 (3H, s, H-24), 0.81 (3H, s, H-28), 0.82 (3H, s, H-25), 0.92 (3H, s, H-27), 0.96 (3H, s, H-26), 1.01

(3H, s, H-23), 1.30-1.19 (5H, m), 1.38 (4H, *br* s), 1.52-1.41 (5H, m), 1.55 (3H, *br* s), 1.70-1.60 (5H, m), 2.15 (1H, t, *J* = 11.1 Hz, H-21a), 2.75 (1H, ddd, *J* = 10.9, 10.9, 5.6 Hz H-19), 3.17 (1H, dd, *J* = 10.6, 5.3 Hz, H-3), 5.90 (1H, *br* s, H-29b), 6.28 (1H, *br* s, H-29a), 9.51 (1H, s, H-30); ^{13}C NMR (75 MHz, $CDCl_3$) δ 195.2 (C-30), 157.4 (C-20), 133.3 (C-29), 79.1 (C-3), 55.4 (C-5), 50.4 (C-9, C-18), 43.4 (C-17), 42.8 (C-14), 40.9 (C-8), 40.1 (C-22), 39.0 (C-4), 38.9 (C-1), 37.9 (C-13), 37.3 (C-10, C-19), 35.5 (C-16), 34.4 (C-7), 28.1 (C-21, C-23), 27.5 (C-2, C-12), 27.5 (C-15), 21.1 (C-11), 18.5 (C-6), 17.9 (C-28), 16.2 (C-25), 16.1 (C-26), 15.5 (C-24), 14.6 (C-27).

*4.5 Preparation of 3-oxo-lup-20(29)-en-30-al (**6**)*

Compound **6** was prepared from **5** (15.0 mg, 0.03 mmol) following the same procedure described for the preparation of **2**. The crude material was chromatographed over flash silica gel with hexane/AcOEt (9.5:0.5) to afford 7.9 mg (53%) of compound **6** as a white amorphous solid. Spectroscopic and spectrometric data of **6** were identical to those reported by Mutai *et al* [11]. ^{1}H NMR (300 MHz, $CDCl_3$) δ 0.83 (3H, s, H-28), 0.91 (3H, s, H-25), 0.93 (3H, s, H-27), 1.02 (3H, s, H-24), 1.05 (3H, s, H-23), 1.06 (3H, s, H-26), 1.08 (2H, *br* s), 1.54-1.25 (15H, m), 1.56 (2H, m), 1.76-1.62 (4H, m), 1.87 (1H, ddd, *J* = 13.2, 7.5, 4.4 Hz, H-1a), 2.50-2.37 (2H, m), 2.76 (1H, ddd, *J* = 10.9, 10.7, 5.8 Hz, H-19), 5.91 (1H, *br* s, H-29b), 6.28 (1H, *br* s, H-29a), 9.51 (1H, s, H-30); ^{13}C NMR (75 MHz, $CDCl_3$) δ 218.2 (C-3), 195.2 (C-30), 157.3 (C-20), 133.3 (C-29), 55.1 (C-5), 49.8 (C-9, C-18), 47.5 (C-4), 43.4 (C-14), 42.9 (C-17), 40.9 (C-8), 40.1 (C-22), 39.8 (C-1), 38.0 (C-13, C-19), 37.0 (C-10), 35.5 (C-16), 34.3 (C-2), 33.7 (C-7), 27.5 (C-12, C-15), 26.7 (C-21, C-23), 21.6 (C-11), 21.2 (C-24), 19.8 (C-6), 17.9 (C-28), 16.0 (C-25), 15.9 (C-26), 14.5 (C-27).

*4.7 Preparation of 3β,16β-dihydroxy-lup-20(29)-en-30-al (**7**)*

Compound **7** was prepared from **1** (60.0 mg, 0.14 mmol) following the same procedure described for the preparation of **5**. The crude material was chromatographed over flash silica gel with hexane/AcOEt (7:3) to afford 59.8 mg (97%) of compound **7** as a white crystalline solid.

Spectroscopic and spectrometric data of **7** were in agreement with those previously reported by our group [7]. ^{1}H NMR (300 MHz, $CDCl_3$) δ 0.74 (3H, s, H-24), 0.79 (3H, s, H-28), 0.81 (3H, s, H-26), 0.95 (3H, s, H-25), 0.95 (3H, s, H-27), 1.00 (3H, s, H-23), 2.85 (1H, ddd, *J* = 5.7, 10.5, 10.8 Hz, H-19), 3.15 (1H, dd, *J* = 5.1, 10.5 Hz, H-3), 3.66 (1H, dd, *J* = 4.8, 11.1 Hz, H-16), 5.91 (1H, br s, H-29a), 6.27 (1H, br s, H-29b), 9.5 (1H, s, H-30); ^{13}C NMR (75 MHz, $CDCl_3$) δ 195.0 (C-30), 156.4 (C-20), 133.5 (C-29), 79.0 (C-3), 77.0 (C-16), 55.4 (C-5), 49.9 (C-9, C-18), 48.9 (C-17), 44.0 (C-14), 41.0 (C-8), 39.0 (C-4), 38.8 (C-1), 37.8 (C-22), 37.2 (C-10), 37.1 (C-13, C-19), 37.0 (C-15), 34.3 (C-7), 29.8 (C-21), 28.1 (C-23), 27.4 (C-2), 27.2 (C-12), 21.0 (C-11), 18.4 (C-6), 16.2 (C-26), 16.1 (C-25, C-27), 15.5 (C-24), 11.7 (C-28).

*4.8 Preparation of 3,16-dioxo-lup-20(29)-ene (**8**)*

Compound **8** was prepared from **1** (50.0 mg, 0.11 mmol) following the same procedure described for the preparation of **2**. The crude material was chromatographed over flash silica gel with hexane/AcOEt (9:1) to afford 20.8 mg (42%) of compound **8** as a white amorphous solid. Spectroscopic and spectrometric data of **8** were in agreement with those previously reported by our group [7]. ^{1}H NMR (400 MHz, $CDCl_3$) δ 0.90 (3H, s, H-27), 0.93 (3H, s, H-25), 1.01 (3H, s, H-24), 1.06 (3H, s, H-23), 1.09 (3H, s, H-28), 1.14 (3H, s, H-26), 1.65 (3H, s, H-30), 2.61 (1H, ddd, *J* = 6.3, 10.8, 10.9 Hz, H-19), 2.71 (1H, d, *J* = 13.6 Hz, H-15a), 4.62 (1H, *br* s, H-29a), 4.73 (1H, *br* s, H-29b); ^{13}C NMR (100 MHz, $CDCl_3$) δ 217.8 (C-3), 215.8 (C16), 148.8 (C-20), 110.8 (C-29), 56.7 (C-17), 54.8 (C-5), 49.4 (C-9), 49.4 (C-18), 48.1 (C-14), 47.4 (C-4, C-19), 44.9 (C-15), 41.0 (C-8), 39.6 (C-1), 37.7 (C-13), 36.9 (C-10), 34.1 (C-2), 33.6 (C-7), 31.2 (C-22), 28.6 (C-21), 26.8 (C-23), 24.8 (C-12), 21.3 (C-11), 21.1 (C-24), 19.7 (C-6), 19.0 (C-30), 18.1 (C-28), 16.3 (C-26), 16.0 (C-25), 15.4 (C-27).

*4.9 Preparation of 3β-hydroxy-lup-20(29)-en-16-one (**9**) and 16β-hydroxy-lup-20(29)-en-3-one (**10**)*

Compounds **9** and **10** were prepared from **1** (50.0 mg, 0.11 mmol) following the procedure described for the preparation of **2**, with minor modifications. Jones reagent was added

dropwise at 0 °C until the appearance of the ketones **9** and **10** was confirmed by TLC, and there was no evidence of the presence of diketone **8**. The crude material was chromatographed over flash silica gel with hexane/AcOEt (9.3:0.7) to afford 8.7 mg (17%) of compound **9** and 7.6 mg (15%) of compound **10** as white amorphous solids.

Compound **9**: ^{1}H NMR (300 MHz, $CDCl_3$) δ 0.68 (1H, d, J = 9.5 Hz, H-5), 0.77 (3H, s, H-24), 0.85 (3H, s, H-25), 0.90 (3H, s, H-27), 0.97 (3H, s, H-23), 1.10 (3H, s, H-28), 1.11 (3H, s, H-26), 1.44-1.36 (8H, m), 1.61- 1.54 (9H, m), 1.66 (3H, s, H-30), 1.83-1.86 (3H, m), 2.12 (1H, ddd, J = 12.5, 12.0, 4.1 Hz, H-13), 2.61 (1H, ddd, J = 11.3, 10.9, 6.0 Hz, H-19), 2.71 (1H, d, J = 13.9 Hz, H-15a), 3.19 (1 H, dd, J = 10.9, 5.2 Hz, H-3), 4.63 (1H, *br* s, H-29b), 4.74 (1H, *br* s, H-29a); ^{13}C NMR (75 MHz, $CDCl_3$) δ 216.1 (C-16), 148.9 (C-20), 110.8 (C-29), 79.0 (C-3), 56.7 (C-5), 55.3 (C-17), 50.1 (C-9), 49.6 (C-18), 48.2 (C-14), 47.5 (C-19), 45.0 (C-15), 41.2 (C-8), 39.0 (C-1), 38.9 (C-4), 37.6 (C- 13), 37.3 (C-10), 34.3 (C-7), 31.3 (C-22), 28.7 (C-21), 28.1 (C-23), 27.5 (C-2), 24.8 (C-12), 20.8 (C-11), 19.1 (C-30), 18.4 (C-6), 18.1 (C-28), 16.6 (C-26), 16.1 (C-25), 15.5 (C-24), 15.5 (C-27); MS (ESI, positive ions), *m/z* 441.4 $[M+H]^+$. Anal. Calcd. for $C_{30}H_{48}O_2$: C 81.76; H 10.98. Found: C 81.81; H 11.03.

Compound **10**: ^{1}H NMR (300 MHz, $CDCl_3$) δ 0.80 (3H, s, H-28), 0.93 (3H, s, H-26), 1.00 (3H, s, H-25), 1.02 (3H, s, H-24), 1.07 (6H, s, H-23, H-27), 1.68 (3H, s, H-30), 1.53-1.26 (17H, m), 2.04-1.89 (3H, m), 2.50-2.42 (3H, m), 3.61 (1H, dd, J = 10.6, 4.7 Hz, H-16), 4.60 (1H, *br* s, H-29b), 4.71 (1H, *br* s, H-29a); ^{13}C NMR (75 MHz, $CDCl_3$) δ 218.2 (C-3), 150.0 (C-20), 110.0 (C- 29), 77.2 (C-16), 55.1 (C-5), 49.5 (C-9), 48.8 (C-17), 47.8 (C-18), 47.7 (C- 19), 47.5 (C-4), 44.3 (C-14), 41.0 (C-8), 39.8 (C-1), 37.8 (C-22), 37.5 (C-13), 37.0 (C-10), 37.0 (C-15), 34.2 (C-2), 33.7 (C-7), 30.0 (C-21), 26.8 (C-23), 24.9 (C-12), 21.5 (C-11), 21.2 (C-24), 19.8 (C-6), 19.5 (C-30), 16.2 (C-25), 16.1 (C-27), 15.9 (C-26), 11.8 (C-28); MS (ESI, positive ions), *m/z* 463.4 $[M+Na]^+$. Anal. Calcd. for $C_{30}H_{48}O_2$: C 81.76; H 10.98. Found: C 81.82; H 11.01.

*4.10 Preparation of 3β-hydroxy-16-oxo-lup-20(29)-en-30-al (**11**)*

Compound **11** was prepared from **9** (14.0 mg, 0.03 mmol) following the same procedure described for the preparation of **5**. The crude material was chromatographed over flash silica gel with hexane/AcOEt (7:3) to afford 6.8 mg (47%) of compound **11** as a white amorphous solid. ^{1}H NMR (300 MHz, $CDCl_3$) δ 0.66 (1H, d, J = 10,2 Hz, H-5), 0.76 (3H, s, H-24), 0.83 (3H, s, H-25), 0.88 (3H, s, H-27), 0.97 (3H, s, H-23), 1.09 (3H, s, H-28), 1.13 (3H, s, H-26), 1.26 (3H, s), 1.44-1.34 (4H, m), 1.73-1.45 (8H, m), 1.82 (1H, d, J = 14.4 Hz, H-15b), 2.06-1.87 (2H, m), 2.17- 2.08 (2H, m), 2.73 (1H, d, J = 13.8 Hz, H-15a), 2.99 (1H, ddd, J = 10.9, 10.8, 6.0 Hz, H-19), 3.17 (1H, dd, J = 10.6, 4.9 Hz, H-3), 5.97 (1H, *br* s, H-29b), 6.28 (1H, *br* s, H-29a), 9.52 (1H, s, H-30); ^{13}C NMR (75 MHz, $CDCl_3$) δ 215.5 (C-16), 194.7 (C-30), 156.5 (C-20), 132.4 (C-29), 79.0 (C-3), 56.9 (C-5), 55.3 (C-17), 49.9 (C-9, C-18), 47.8 (C-14), 45.0 (C-15), 41.1 (C-8), 39.0 (C-1), 38.8 (C-4), 37.3 (C-13), 37.2 (C-10, C-19), 34.3 (C-7), 31.3 (C-22), 29.8 (C-21), 28.1 (C-23), 27.5 (C-2), 27.1 (C-12), 20.8 (C-11), 18.3 (C- 6), 18.0 (C-28), 16.5 (C-26), 16.1 (C-25), 15.5 (C-24), 15.4 (C-27); MS (ESI, positive ions), *m/z* 477.4 $[M+Na]^+$. Anal. Calcd. for $C_{30}H_{46}O_3$: C 79.25; H 10.20. Found: C 79.28; H 10.23.

*4.11 Preparation of 16β-hydroxy-3-oxo-lup-20(29)-en-30-al (**12**) and 16β-hydroxy-3-oxo-lup-1,20(29)-dien-30-al (**13**)*

Compound **12** and **13** were prepared from **10** (7.8 mg, 0.02 mmol) following the same procedure described for the preparation of **5**. The crude material was chromatographed over flash silica gel with hexane/AcOEt (8.5:1.5/8.3:1.7) to afford 1.1 mg (14%) of compound **12** and 1.5 mg (19%) of compound **13**.

Compound **12:** ^{1}H NMR (300 MHz, $CDCl_3$) δ 0.83 (3H, s, H-28), 0.92 (3H, s, H-26), 0.98 (3H, s, H-25), 1.02 (3H, s, H-27), 1.06 (3H, s, H-24), 1.07 (3H, s, H-23), 1.74-1.26 (20H, m), 2.47-2.40 (2H, m, H-2), 2.86 (1H, ddd, J = 10.8, 10.5, 5.7 Hz, H-19), 3.69 (1H, dd, J = 11.2, 4.8 Hz, H-16), 5.93 (1H, *br* s, H-29b), 6.29 (1H, *br* s, H-29a), 9.52 (1H, s, H-30); ^{13}C NMR (75 MHz, $CDCl_3$) δ 217.9 (C-3), 195.0 (C-30), 156.9 (C-20), 133.0 (C-29), 76.9 (C-16), 53.5 (C-5), 49.2 (C-9, C-17, C-18), 44.8 (C-4), 44.1 (C-14), 41.9 (C-8), 39.7 (C-1), 37.9 (C-22), 37.1 (C-13, C-19), 37.0 (C-10), 36.9 (C-15), 34.2 (C-2), 33.6 (C-7), 31.7 (C-21), 27.1 (C-12), 26.7 (C-23),

21.3 (C-11), 21.1 (C-24), 19.7 (C-6), 16.0 (C-25), 15.8 (C-27), 15.8 (C-26), 11.7 (C-28); MS (ESI, positive ions), *m/z* 455.4 $[M+H]^+$. Anal. Calcd. for $C_{30}H_{46}O_3$: C 79.25; H 10.20. Found: C 79.30; H 10.24.

Compound **13**: ^{1}H NMR (300 MHz, $CDCl_3$) δ 0.85 (3H, s, H- 28), 0.96 (3H, s, H-27), 1.05 (3H, s, H-25), 1.08 (3H, s, H-24), 1.10 (3H, s, H-26), 1.13 (3H, s, H-23), 2.00-1.26 (16H, m), 2.94-2.82 (1H, m, H-19), 3.69 (1H, dd, *J* = 11.2, 4.8 Hz, H-16), 5.78 (1H, d, *J* = 10.2 Hz, H-2), 5.95 (1H, *br* s, H-29b), 6.30 (1H, *br* s, H-29a), 7.05 (1H, d, *J* = 10.2 Hz, H-1), 9.53 (1H, s, H-30); ^{13}C NMR (75 Hz, $CDCl_3$) δ 205.5 (C-3), 195.0 (C-30), 159.5 (C-1), 156.2 (C-20), 133.5 (C-29), 125.4 (C-2), 76.9 (C-16), 53.6 (C-5), 49.0 (C-17, C-18), 44.8 (C-4), 44.2 (C-9), 44.1 (C-14), 41.9 (C-8), 39.6 (C-10), 37.9 (C-22), 37.3 (C-13, C-19), 36.9 (C-15), 33.9 (C-7), 31.7 (C-21), 27.9 (C-23), 27.1 (C-12), 21.5 (C-24), 21.3 (C-11), 19.3 (C-25), 19.1 (C-6), 16.6 (C-26), 14.3 (C-27), 11.8 (C-28); MS (ESI, positive ions), *m/z* 453.4 $[M+H]^+$. Anal. Calcd. for $C_{30}H_{44}O_3$: C 79.60; H 9.80. Found: C 79.64; H 9.85.

4.12 Inhibition assay on AChE and BChE in vitro

Electric eel (*Torpedo californica*) AChE and horse serum BChE were used as source of both the cholinesterases. AChE and BChE inhibiting activities were measured *in vitro* by the spectrophotometric method developed by Ellman with slight modification [19]. The lyophilized enzyme, 500U AChE/300U BChE, was prepared in buffer A (8 mM K_2HPO_4, 2.3 mM NaH_2PO_4) to obtain 5/3 U/mL stock solution. Further enzyme dilution was carried out with buffer B (8mM K_2HPO_4, 2.3 mM NaH_2PO_4, 0.15 M NaCl, 0.05% Tween 20, pH 7.6) to produce 0.126/0.06 U/mL enzyme solution. Samples were dissolved in buffer B with 2.5% of MeOH as cosolvent. Enzyme solution (300 µL) and sample solution (300 µL) were mixed in a test tube and incubated for 60/120 min at room temperature. The reaction was started by adding 600 µL of the substrate solution (0.5 mM DTNB, 0.6 mM ATCI/BTCI, 0.1 M Na_2HPO_4, pH 7.5). The absorbance was read at 405 nm for 180 s at 27ºC. Enzyme activity was calculated by comparing reaction rates for the sample to the blank. All the reactions were performed in triplicate. IC_{50}

values were determined with GraphPad Prism 5. Tacrine (99%) was used as reference AChE/BChE inhibitor.

4.13 Kinetic characterization of BChE inhibition

The enzyme reaction was carried out at three fixed inhibitor concentrations (0, 20 and 70 μM for compound **2**; 0, 10 and 75 μM for compound **9**). In each case the initial velocity measurements were obtained at varying substrate (S) (butyrylthiocholine) concentrations and the reciprocal of the initial velocity (1/v) was plotted as a function of the reciprocal of [S] (1/[S]). The double-reciprocal (Lineweaver–Burk) plot showed a pattern of intersecting lines with increasing slopes, characteristic of a competitive inhibitor. The data of the enzyme activity at different fixed substrate concentrations with increasing inhibitor concentrations were analyzed with GraphPad Prism 5. The nonlinear regression of these data fitted with competitive inhibition with R^2= 0.9836 for **2** and R^2= 0.9802 for **9**. The calculated K_i were 51.16 μM for **9** and 32.70 μM for **2**.

4.14 Molecular docking determinations

Human BChE crystal structure 1P0I [22] and *Torpedo californica* AChE crystal 2ACE [23] were used for the docking simulations of compounds **2** and **9**. Due to both compounds are competitive inhibitors, the acetylcholine was not present at their active site. Geometry optimization of the compounds was performed with semiempirical calculations (AM1) and the Hartree-Fock method and the 6-31G (d, p) basis set incorporated in the Gaussian 03 program [24-26]. Docking studies were performed with version 4.2.5.1 of the program AutoDock, using the implemented empirical free energy function [21, 27]. The graphical user interface program AutoDock Tools was used to prepare, run and analyze the docking simulations. The simulation space was defined as box which included the active site and the peripheral site. Atomic interaction energy on a 0.375 Å grid was calculated with the auxiliary program Autogrid 4 using probes corresponding to each map type found in the inhibitor. All rotatable dihedrals in both

compounds were allowed to rotate freely. The starting position of the triterpene was outside the grid on a random position.

The triterpenes were docked by the Lamarckian genetic algorithm protocol. A total of 256 independent simulations with a population size of 150 members were run for each compound using AutoDock 4.2.5.1 with default parameters (random starting position and conformation, translation step of 2.0 Å, mutation rate of 0.02, crossover rate of 0.8, local search rate 0.06 and 2500000 energy evaluations). After docking, the 256 conformers generated for the inhibitors were assigned to clusters based on a tolerance of 2.0 Å all atom root-mean-square deviation (rmsd) in position from the lowest-energy solution. The clusters were also ranked according to the energies of their representative conformations, which were the lowest-energy solutions within each cluster.

Acknowledgments

This work was financially supported by Consejo Nacional de Investigaciones Científicas y Técnicas (CONICET), Universidad Nacional del Sur and Comisión de Investigaciones Científica (CIC) from Argentina. M.J.C. and V.R. are grateful to CONICET for their postdoctoral fellowships. M.B.F. is a Research Member of CIC. A.P.M. and V.R. are Research Members of CONICET.

Appendix A. Supplementary material

Supplementary data associated with this article can be found, in the online version, at ……

References

[1] Bachurin SO, Bovina EV, Ustyugov AA. Drugs in Clinical Trials for Alzheimer's Disease: The Major Trends. *Med Res Rev.* 2017, 37:1186–1225.

[2] Cummings J, Lee G, Mortsdorf T, Ritter A, Zhong K. Alzheimer's disease drug development pipeline: 2017. *Alzheimers Dement.* 2017, 3:367–384.

[3] Lanctôt KL, Amatniek J, Ancoli-Israel S, Arnold SE, Ballard C, Cohen-Mansfield J, Ismail Z, Lyketsos C, Miller DS, Musiek E, Osorio RS, Rosenberg PB, Satlin A, Steffens D, Tariot P, Bain LJ, Carrillo MC, Hendrix JA, Jurgens H, Boot B. Neuropsychiatric signs and symptoms of Alzheimer's disease: New treatment paradigms. *Alzheimers Dement.* 2017, 3:440–449.

[4] Huff FJ, Reiter CT, Rand JBJ. The ratio of acetylcholinesterase to butyrylcholinesterase influences the specificity of assays for each enzyme in human brain. *J. Neural Transm.* 1989, 75: 129–134.

[5] Dvir H, Silman I, Harel M, Rosenberry TL, Sussman JL. Acetylcholinesterase: From 3D structure to function. *Chem. Biol. Interact.* 2010, 187:10–22.

[6] Nordberg A, Ballard C, Bullok R, Darreh-Shori T, Somogvi M. A review of butyrylcholinesterase as a therapeutic target in the treatment of Alzheimer's disease. *Prim. Care Companion J. Clin. Phys.* 2013, 15: PCC.12r01412.

[7] Castro MJ, Richmond V, Romero C, Maier MS, Estévez-Braun A, Ravelo AG, Faraoni MB, Murray AP. Preparation, anticholinesterase activity and molecular docking of new lupane derivatives. *Bioorg Med Chem.* 2014, 22:3341–3350.

[8] Vela Gurovic MS, Castro MJ, Richmond V, Faraoni MB, Maier MS, Murray AP. Triterpenoids with acetylcholinesterase inhibition from *Chuquiraga erinacea* D. Don. subsp. *erinacea* (Asteraceae). *Planta Med.* 2010, 76:607–610.

[9] Gutiérrez-Nicolás F, Gordillo-Román B, Oberti JC, Estévez-Braun A, Ravelo AG, Joseph-Nathan P. Synthesis and Anti-HIV Activity of Lupane and Olean-18-ene Derivatives. Absolute Configuration of 19,20-Epoxylupanes by VCD. *J Nat Prod.* 2012, 75:669–676.

[10] Khan MF, Maurya CK, Dev K, Arha D, Rai K, Tamrakar AK, Maurya R. Design and synthesis of lupeol analogues and their in vitro PTP-1B inhibitory activity. *Bioorg Med Chem Lett.* 2014, 24:2674–2679.

[11] Mutai C, Abatis D, Vagias C, Moreauc D, Roussakisc C, Roussis V. Lupane Triterpenoids from *Acacia mellifera* with Cytotoxic Activity. *Phytochemistry.* 2004, 65:1159–1164.

[12] Prachayasittikul S, Saraban P, Cherdtrakulkiat R, Ruchirawat S, Prachayasittikul V. New bioactive triterpenoids and antimalarial activity of *Diospyros rubra* lec. *Excli J.* 2010, 9:1–10.

[13] Bhandari P, Patel NK, Bhutani KK. Synthesis of new heterocyclic lupeol derivatives as nitric oxide and pro-inflammatory cytokine inhibitors. *Bioorg Med Chem Lett*. 2014, 24:3596–3599.

[14] Yasukawa K, Yu SY, Yamanouchi S, Takido M, Akihisa T, Tamura T. Some lupane-type triterpenes inhibit tumor promotion by 12-0-tetradecanoylphorbol-13-acetate in two-stage carcinogenesis in mouse skin. *Phytomedicine*. 1995, 1:309–313.

[15] Khan MF, Mishra DP, Ramakrishna E, Rawat AK, Mishra A, Srivastava AK, Maurya R. Design and synthesis of lupeol analogues and their glucose uptake stimulatory effect in L6 skeletal muscle cells. *Med Chem Res.* 2014, 23:4156–4166.

[16] Burns D, Reynolds WF, Buchanan G, Reese PB, Enriquez RG. Assignment of ^{1}H and ^{13}C spectra and investigation of hindered side-chain rotation in lupeol derivatives. *Magn Reson Chem.* 2000, 38:488–493.

[17] Pech GG, Brito WF, Mena GJ, Quijano L. Constituents of *Acacia cedilloi* and *Acacia gaumeri*. Revised structure and complete NMR assignments of resinone. *Z Naturforsch C.* 2002, 57:773–776.

[18] Wei Y, Ma C, Chen D, Hattori M. Anti-HIV-1 protease triterpenoids from *Stauntonia obovatifoliola* Hayata subsp. *intermedia*. *Phytochemistry*. 2008, 69:1875–1879.

[19] Ellman GL, Courtney KD, Andres V, Featherstone RM. A new and rapid colorimetric determination of acetylcholinesterase activity. *Biochem Pharmacol.* 1961, 7:88–95.

[20] Saxena A, Redman AM, Jiang X, Lockridge O, Doctor BP. Differences in active-site gorge dimensions of cholinesterases revealed by binding of inhibitors to human butyrylcholinesterase. *Chem Biol Interact.* 1999, 119-120:61–69.

[21] Forli S, Olson AJ. Force field with discrete displaceable waters and desolvation entropy for hydrated ligand docking. *J Med Chem.* 2012, 55:623–638.

[22] Nicolet Y, Lockridge O, Masson P, Fontecilla-Camps JC, Nachon F. Crystal characterization of human butyrylcholinesterase and of its complexes with substrate and products. *J Biol Chem.* 2003, 278:41141–41147.

[23] Raves ML, Harel M, Pang YP, Silman I, Kozikowski AP, Sussman JL. Structure of acetylcholinesterase complexed with the nootropic alkaloid, (-)-huperzine A. *Nat Struct Biol.* 1997, 4:57–63.

[24] Dewar MJS, Zoebisch EG, Healy EF, Stewart JJP. Development and use of quantum mechanical molecular models. 76. AM1: a new general purpose quantum mechanical molecular model. *J Am Chem Soc*. 1985, 107:3902–3909.

[25] Roothaan CCJ. New Developments in Molecular Orbital Theory. *Rev Mod Phys.* 1951, 23:69–89.

[26] Gaussian 03, Revision C.01, Frisch MJ, Trucks GW, Schlegel HB, Scuseria GE, Robb MA, Cheeseman JR, Montgomery JA, Vreven T, Kudin KN, Burant JC, Millam JM, Iyengar SS, Tomasi J, Barone V, Mennucci B, Cossi M, Scalmani G, Rega N, Petersson GA, Nakatsuji H, Hada M, Ehara M, Toyota K, Fukuda R, Hasegawa J, Ishida M, Nakajima T, Honda Y, Kitao O, Nakai H, Klene M, Li X, Knox JE, Hratchian HP, Cross JB, Bakken V, Adamo C, Jaramillo J, Gomperts R, Stratmann, RE, Yazyev O, Austin AJ, Cammi R, Pomelli C, Ochterski JW, Ayala PY, Morokuma K, Voth GA, Salvador P, Dannenberg JJ, Zakrzewski VG, Dapprich S, Daniels AD, Strain MC, Farkas O, Malick DK, Rabuck AD, Raghavachari K, Foresman JB, Ortiz JV, Cui Q, Baboul AG, Clifford S, Cioslowski J, Stefanov BB, Liu G, Liashenko A, Piskorz P, Komaromi I, Martin RL, Fox DJ, Keith T, Al-Laham MA, Peng CY, Nanayakkara A, Challacombe M, Gill PMW, Johnson B, Chen W, Wong MW, Gonzalez C, Pople JA, Gaussian Inc., Wallingford CT, 2004.

[27] Auto-Dock 4.2 The Scripps Research Institute, Department of Molecular Biology, MB-5, La Jolla, CA, 2013.

Graphical Abstract

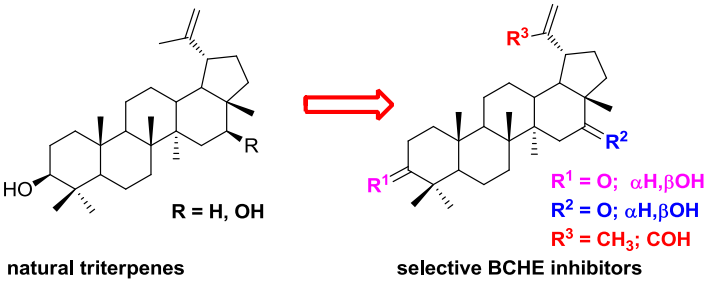

natural triterpenes

selective BCHE inhibitors

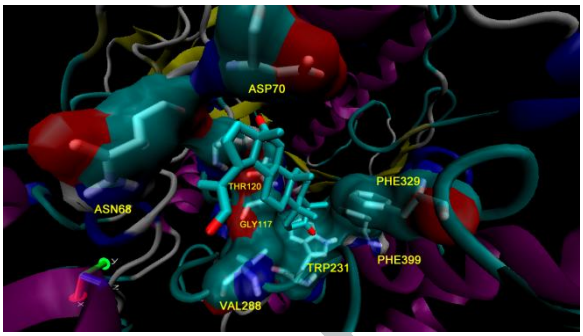

Highlights

- A set of mono-, di- and tri-oxolupanes were prepared starting from calenduladiol and lupeol.
- Selective inhibition of butyrylcholinesterase was observed for all the derivatives.
- Kinetic study and molecular modeling were carried with the most potent inhibitors.
- Oxidation at C-16 of the lupane skeleton improves the cholinesterase inhibition.